Research Article | Vol. 27, No. 6 | 18 Mar 2019 | OPTICS EXPRESS 8792
Optics EXPRESS

Frequency modulated free electron laser

L. T. CAMPBELL[1,2,3,4] AND B. W. J. MCNEIL[1,3,*]

[1]SUPA, Department of Physics, University of Strathclyde, Glasgow G4 0NG, UK
[2]ASTeC, STFC Daresbury Laboratory, Warrington WA4 4AD, UK
[3]Cockcroft Institute, Warrington WA4 4AD, UK
[4]lawrence.campbell@strath.ac.uk
[*]b.w.j.mcneil@strath.ac.uk

Abstract: It is shown that the output frequency of a free electron laser may be modulated to generate a series of modes that span a bandwidth of at least an order of magnitude greater than the normal FEL bandwidth. This new method of frequency modulated FEL operation has close analogies to frequency modulation in conventional cavity lasers. The FM-FEL is analysed and described in the linear regime by a summation over the exponentially amplified frequency modes. Simulations using a 3D, broad bandwidth, numerical code also demonstrate FM-FEL operation for parameters typical of FEL facilities currently under construction. Harmonic bunching methods are used to seed the FM-FEL modes to generate a temporally correlated frequency modulated output over a large bandwidth. This new, FM-FEL mode of operation scales well for X-ray generation, offering users a significantly new form of high-power, short wavelength FEL output.

1. Introduction

Free Electron Laser (FEL) is currently the world's brightest source of X-rays by many orders of magnitude [1–3]. The FEL consists of a relativistic electron beam injected through a magnetic undulator with a co-propagating resonant radiation field. Initially, co-propagating radiation will occur due to incoherent spontaneous noise emission from the electron beam and may be supplemented by an injected seed laser. The electrons can interact cooperatively with the radiation they emit and become density modulated at the resonant radiation wavelength. This coherently modulated oscillating electron beam exponentially amplifies the co-propagating radiation field in a positive feedback loop. In the single-pass high-gain mode, the energy of the initial incoherent, spontaneous X-rays may be amplified by around ten orders of magnitude. With such an increase in brightness over other laboratory sources, the X-ray FEL has unique applications across a wide range of the natural sciences. FEL science is, however, still under development, and the creation of novel and improved output from the FEL is still an active topic of research.

For example, it has been shown via simulations that equally spaced frequency modes may be generated in a single-pass FEL amplifier [4, 5] by introducing a series of delays to the electron beam with respect to the co-propagating radiation field (e.g. by using magnetic chicanes placed between undulator modules). These radiation modes are formally identical to those created in an oscillator cavity. Analogously with a mode-locked conventional laser oscillator, a modulation of the electron beam energy [4, 5] or current [6] at the mode spacing can phase-lock the modes and amplify them to generate a train of short, high power pulses.

Multiple colours may also be excited by directly tuning each undulator module to switch between 2 (or more) distinct colours [7]. This colour switching may also excite and amplify modes via a resulting gain modulation [8].

2. Frequency modulated FEL model

The FEL resonant frequency ω_r can be tuned via the electron beam energy γ_0, the undulator period λ_u and the undulator magnetic field strength B_u, via the resonance relation $\omega_r = 2\gamma_0^2 c k_u/(1+\bar{a}_u^2)$,

#358201 https://doi.org/10.1364/OE.27.008792
Journal © 2019 Received 22 Jan 2019; revised 1 Mar 2019; accepted 1 Mar 2019; published 11 Mar 2019

Optics EXPRESS

where $k_u = 2\pi/\lambda_u$ and the RMS undulator parameter $\bar{a}_u \propto B_u\lambda_u$. In the following, the resonant frequency of the FEL is periodically modulated by modulating the magnetic undulator field. This excites a Bessel-like modal radiation output with a corresponding temporal-frequency modulation and with the modal spacing being much greater than the normal FEL amplification bandwidth.

The undulator parameter is modulated via its magnetic field so that $\bar{a}_u(\bar{z}) = \bar{a}_{u0}(1 + \epsilon(\bar{z}))$, where $\bar{z} = z/l_g$ is the propagation distance through the undulator scaled with respect to the FEL gain length $l_g = \lambda_u/4\pi\rho$, and ρ is the FEL parameter [9]. Using $\epsilon(\bar{z}) = \kappa\sin(\bar{k}_M\bar{z})/2$, and in the limit $\bar{a}_{u0} \gg 1$ and $\kappa \ll 1$, the resonant frequency is then sinusoidally modulated around the carrier frequency ω_{r0} as $\omega_r = \omega_{r0}(1 - \kappa\sin(k_M\bar{z}))$.

As with frequency modulation (FM) in conventional cavity lasers or radio transmission [10], a modulation index $\mu = \kappa/(2\rho\bar{k}_M)$ may be defined. This is the ratio of the frequency modulation amplitude to the modulation frequency. The approximate number of modes within the modulation amplitude is then $N_M \approx 2\mu + 1$ [10]. Cases of interest are when $N_M \geq 3$, and the relative mode spacing is greater than the nominal FEL bandwidth, ρ.

A coupled system of linearised equations is derived similar to those of [11] which describe a tapered undulator FEL, but for a periodically modulated helical undulator field, as described above. Unlike [11], the steady state approximation is not applied, as the position dependence within the electron pulse of $\bar{z}_1 = (z - c\bar{\beta}_z t)/\bar{\beta}_z l_c$ [12] is retained, where $\bar{\beta}_z = \bar{v}_z/c$ is the scaled mean electron z-velocity and $l_c = \lambda_{r0}/4\pi\rho$ is the nominal FEL cooperation length. Using the collective, linearised FEL variables as defined in [9] for the electron phase $\theta = \bar{z}_1/2\rho$, bunching $b(\bar{z}, \bar{z}_1)$, scaled electron energy $P(\bar{z}, \bar{z}_1)$, and the scaled, slowly varying complex radiation envelope $A(\bar{z}, \bar{z}_1)$ (the electric field $E_x + iE_y \propto Ae^{i\omega_{r0}(z/c-t)}$), the following linerarised, fourier transformed system of equations can be derived which describe the FEL interaction for electron pulses with a modulated undulator in the linear regime [9]:

$$\frac{\partial\tilde{b}(\bar{z},\bar{\omega})}{\partial\bar{z}} = -i\tilde{P} \tag{1}$$

$$\frac{\partial\tilde{P}(\bar{z},\bar{\omega})}{\partial\bar{z}} = -\tilde{A}e^{-i\theta_{r0}} \tag{2}$$

$$\frac{\partial\tilde{A}(\bar{z},\bar{\omega})}{\partial\bar{z}} = \tilde{b}e^{i\theta_{r0}} - i\bar{\omega}\tilde{A}. \tag{3}$$

Here, the Fourier transform is defined as $\tilde{x}(\bar{\omega}) = 1/\sqrt{2\pi}\int_{-\infty}^{\infty} x(\bar{z}_1)e^{-i\bar{\omega}\bar{z}_1}d\bar{z}_1$, where $\bar{\omega} = (\omega - \omega_{r0})/2\rho\omega_{r0}$ is the scaled radiation frequency in units of the amplification bandwidth ρ. The phase $\theta_{r0}(\bar{z}) = \int_0^{\bar{z}}\epsilon(\bar{z}')d\bar{z}'/\rho$ describes the effect of the phase modulation of the electrons away from the carrier frequency ω_{r0}. For a sinusoidal modulation, the resonant phase modulation is $\theta_{r0} = \mu(1 - \cos(\bar{k}_M\bar{z}))$ and, using the well-known Bessel identity, the resonant phase modulation terms in Eqs. (2)–(3) may be written:

$$e^{i\theta_{r0}} = \sum_{n=-\infty}^{\infty} i^n J_n(\mu)e^{in\bar{k}_M\bar{z}}, \tag{4}$$

where J_n is the n^{th} order Bessel function, which defines the nth mode, and the coupling between the different modes is apparent.

By decoupling the evolution of the electrons from the radiation, by setting and maintaining the spectral bunching at its initial value $\tilde{b}(\bar{z} = 0, \bar{\omega}) = \tilde{b}_0(\bar{\omega})$ for all values of $\bar{z}$, the exact solution for the spontaneously radiated field envelope can be shown to be:

$$\tilde{A}(\bar{z},\bar{\omega}) = \tilde{b}_0(\bar{\omega})M_U(\bar{z},\bar{\omega})\bar{z}, \tag{5}$$

Optics EXPRESS

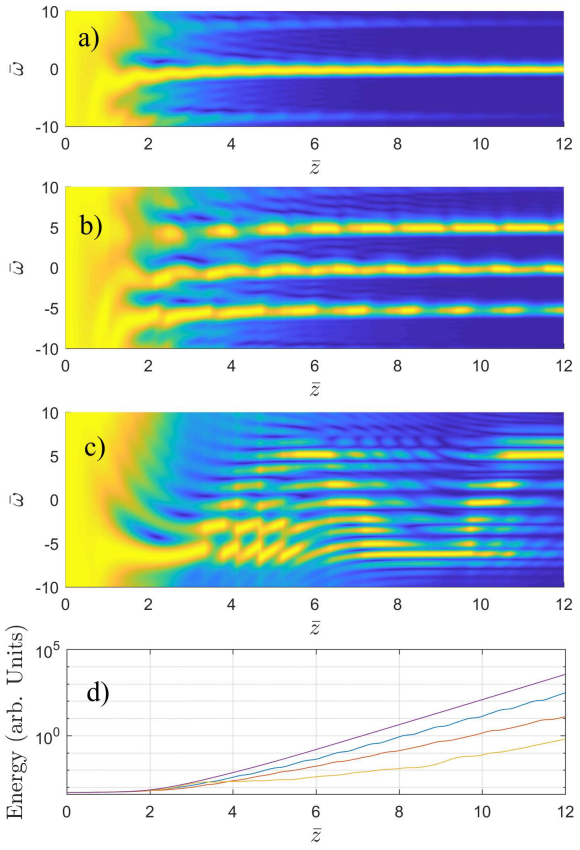

Fig. 1. Numerical solution of the linear FEL Eqs. (1–3) using a sinusoidal frequency modulation with $\kappa = 0.014$ and $\rho = 0.001$. The evolution of the normalised spectral intensity profile of the field is plotted from an initial constant broad bandwidth seed. From the top, and with each vertical slice in $\bar{z}$ normalised to its maximum: a) $\bar{k}_M = 8$; b) $\bar{k}_M = 5$; and c) $\bar{k}_M = 1$ corresponding to modulation index $\mu = 0.875$, 1.4 and 7 respectively. The bottom plot d), shows how the relative total energies integrated over frequency reduce with increasing values of $\mu = 0$, 0.875, 1.4 and 7 respectively.

Optics EXPRESS

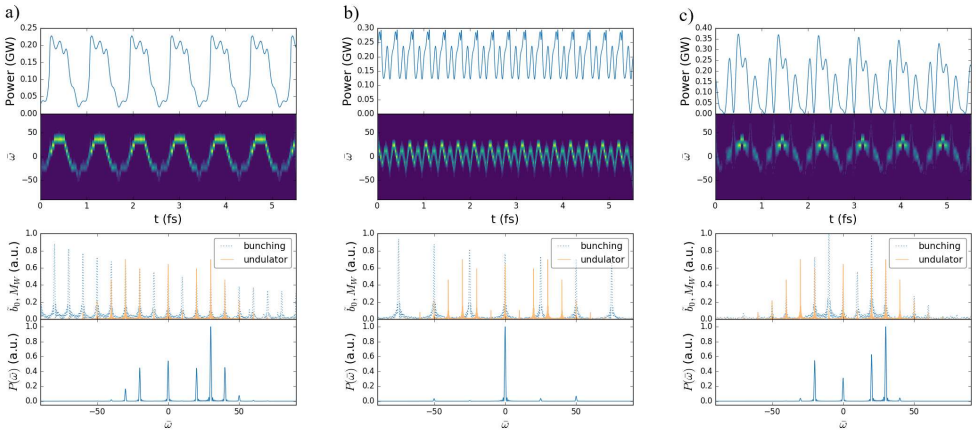

Fig. 2. *a*) 1D Puffin simulation of an HGHG seeded FM FEL. From the top: Radiation output power vs scaled temporal coordinate at saturation, here at $\bar{z} \approx 6.2$; a Synchro-Squeezed Wavelet Transform (SSWT) analysis [16] of the output radiation field showing the temporal-frequency correlation of the radiation output; the spectrum of the electron beam bunching and the FM undulator modes; the radiation power spectrum. *b*) As *a*), but with an HGHG seed of $\lambda_{HG} = 104$nm, corresponding to $\bar{k}_H = 25$ so that the harmonic bunching spectrum now overlaps only the $n = 0$, and ± 1 undulator modes. *c*) As *a*), but now using an EEHG seed, with both lasers tuned to $\lambda_{EE} = 260$nm, and with EEHG chicanes tuned to optimize the bunching around $\lambda_{r0} = 5.2$nm, the 50^{th} harmonic of λ_{EE}.

where, defining $\mathrm{sinc}(x) = \sin(x)/x$:

$$M_U = \sum_{n=-\infty}^{\infty} i^n J_n(\mu) e^{-i(\bar{\omega}-n\bar{k}_M)\bar{z}/2} \,\mathrm{sinc}\left(\frac{(\bar{\omega}+n\bar{k}_M)\bar{z}}{2}\right), \tag{6}$$

is the sum over what are defined as the FM *undulator* modes. For a single electron, or extremely short electron bunch length ($l_b \ll \lambda_{r0}$) as a source, Eq. (5) yields a constant amplitude, sinusoidally frequency modulated signal similar to that generated by an conventional FM laser [10]. For long electron bunches ($l_b > \lambda_{r0}$), where the electrons are uniformly, randomly distributed over each radiation wavelength in the pulse, a clear, temporally correlated frequency modulated radiation output is obscured due to the electron beam shot-noise. The radiation has random, uncorrelated phases for each mode, generating a noisy broadband output.

Defining the envelope of the phase modulated field as $\bar{A} = \tilde{A}e^{i\theta_{r0}}$, and Laplace transforming Eqs. (1)–(3) ($\hat{A}(s,\bar{\omega}) = \mathcal{L}\{\bar{A}(\bar{z},\bar{\omega})\}$, $\hat{b}(s,\bar{\omega}) = \mathcal{L}\{\tilde{b}(\bar{z},\bar{\omega})\}$ etc), a recursive solution of exponential modes, again common to other FM systems in conventional lasers [10], in Laplace space is obtained:

$$\hat{A}_n = \frac{s_n^2}{s_n^2(s_n+\bar{\omega})+1}\left(\frac{\kappa}{4\rho}\left(\hat{A}_{n-1}-\hat{A}_{n+1}\right)-\tilde{A}_0\right), \tag{7}$$

where $s_n \equiv s + n\bar{k}_M$, $\hat{A}_n \equiv \hat{A}(s_n,\bar{\omega})$ and $\tilde{A}_0 \equiv \tilde{A}(\bar{z}=0,\bar{\omega})$. For $\kappa, n = 0$, this modal system reduces to the cubic characteristic equation of the normal, un-modulated undulator FEL [9].

Numerical solutions of the linear system of Eqs. (1)–(3) (note that the linear system does not include saturation effects) are shown in Fig. 1, where multiple modes, corresponding to those of (6), are seen to be amplified over a greatly enhanced bandwidth from that of a normal FEL which has a (scaled) gain bandwidth of $\Delta\bar{\omega} \approx 1$. The gain length is seen to increase with the

Optics EXPRESS

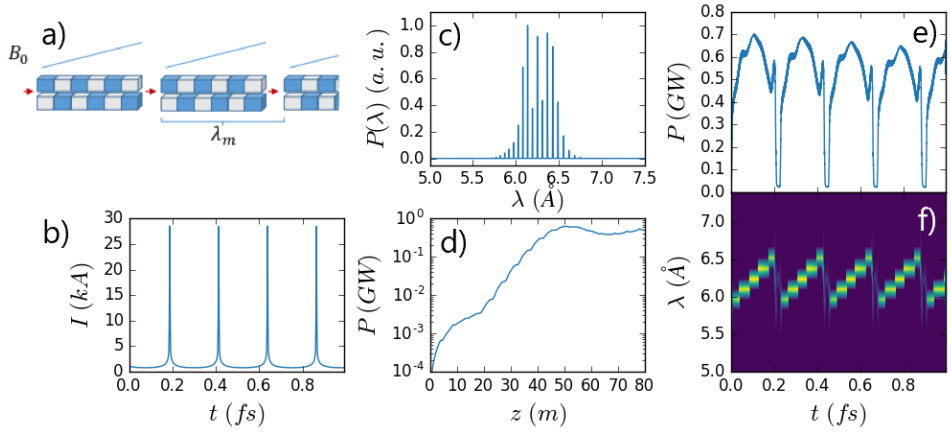

Fig. 3. 3D simulation of a FM-FEL operating in the X-ray. a) Schematic of the undulator line using linearly tapered wiggler modules to periodically modulate the FEL resonant frequency. b) Current profile of the beam, seeded using HGHG. c) Output spectrum of radiation at saturation. d) Radiated power as a function of distance through the undulator. The regions of no growth are the drift regions between undulator modules containing the FODO focussing quadrupoles. e) Temporal power profile at saturation. f) SSWT analysis, showing the temporal-frequency correlation in the on-axis field at saturation.

modulation index μ. For values of $\mu \gtrsim 5$, the saturation length is approximately double that of the usual unmodulated ($\mu = 0$) SASE case.

To generate FM output that possesses a well defined temporal-frequency correlation, the product of the beam bunching $\tilde{b}_0$ and undulator modes M_U of Eq. (5), should have correlated FM phases. This occurs when the beam is bunched coherently with a fixed-phase relationship between the undulator modes M_U. The resultant product of the electron beam bunching spectrum with the undulator modes then possesses a well defined FM phase relationship.

3. FM-FEL simulations

In what follows, the broad bandwidth FEL simulation code Puffin [13] was used in 1D mode with periodic boundary conditions applied, to simulate both High-Gain Harmonic Generation (HGHG) [14] and Echo-Enabled Harmonic Generation (EEHG) [15] schemes that seed the electron beam bunching $\tilde{b}_0(\bar{\omega})$, at phase correlated frequencies corresponding to the undulator modes M_U, of the subsequent modulated undulator system. Figure 2 gives examples of the resultant phase correlated FM output from the modulated undulators for both HGHG and EEGH bunched electron beams. It can be seen that the time correlated FM output bandwidth obtained is up to two orders of magnitude greater than the usual FEL bandwidth. At this stage, no attempt has been made to maximise the FM bandwidth.

A beam current $I = 1.8$kA and energy $E_0 = 5$GeV, with a homogeneous energy spread of $\sigma_E/E_0 = 1 \times 10^{-5}$, was used with undulator period $\lambda_u = 4$cm and mean undulator parameter $\bar{a}_{u0} = 5.0$. This corresponds to a FEL parameter of $\rho = 0.001$, and carrier frequency $\omega_{r0} = 2\pi c/\lambda_{r0}$ with $\lambda_{r0} = 5.2$nm. The undulator has a sinusoidal modulation of the peak magnetic field of period 50 undulator periods, corresponding to $\bar{k}_M = 10$, and modulation index $\mu = 4$. The beam is seeded in the HGHG mode using a laser wavelength $\lambda_H = 260$nm, corresponding to scaled wavenumber $\bar{k}_H = 10$, so that the higher HGHG harmonics occur at the undulator modes of $\omega_{r0} - nck_M$, with ω_{r0} at the 50^{th} harmonic of this seed.

The beam energy spread in this example is small with $\sigma_E/E_0 = 10^{-2}\rho$. The primary aim here

Optics EXPRESS

is to allow for the efficient up-conversion to the 50^{th} harmonic of the HGHG seed in a single stage and is not a requirement for subsequent FM-FEL operation. In a more realistic design, the requirements on the energy spread may mean that the harmonic up-conversion would require to be cascaded in 2 or more stages, as is frequently done at *e.g.* the FERMI facility [17].

In Fig. 2(a), the HGHG seed possesses higher harmonic bunching components overlapping all of the undulator modes with significant power. The FM temporal-frequency correlation is maintained until FEL saturation, at which point the phases of the modes are then seen to drift from the FM phases.

An HGHG example with a higher frequency seed at $\lambda_{HG} = 104$nm is shown in Fig. 2(b). This beam has harmonic bunching components which coincide with only three of the undulator modes. The inherent tunability of the FEL and use of the HGHG seeding method also allows significant variation of the correlations made possible between the seeded beam bunching modes and those of the undulator modes in the same FM-undulator system.

It is noted that EEHG may be more advantageous to use to directly up-convert to a high harmonic in a single stage due to its improved harmonic conversion efficiency. Fig. 2(c) gives an example of an EEHG seed at 260nm, with harmonic bunching components optimized to around the 52^{nd} harmonic, overlapping a sequence of the undulator modes.

While the above examples of a sinusoidally modulated undulator allow for a more elegant analysis, a typical FEL facility undulator line is composed of many identical undulator modules, with free-space drifts between each module to allow for insertion of other beam optical elements such as diagnostic instruments and beam focusing quadrupoles. In this scenario, a more feasible form of the FM-FEL would be to *e.g.* linearly taper each module, resulting in a piecewise discontinuous modulation if the free-space drifts between undulator modules are taken into account. The harmonic seeding should then be at harmonics of the modes defined by the undulator module plus inter-module drift length. Note that the system of Eqs. (1)-(3) still remain valid for such a modulation in the 1D approximation, although in the following example we also model 3D effects to test the robustness of the scheme to effects such as diffraction and a finite electron beam emittance.

A full 3D simulation was performed using Puffin with parameters similar to the SwissFEL Athos undulator line [18], linearly tapering each module as described above, and including focusing quadrupole magnets and free space drifts between the modules. FEL lasing is at carrier wavelength $\lambda_{r0} = 6.25$Å , with each module being linearly tapered from $\bar{a}_u = 0.95 \rightarrow 1.05$, around undulator parameter $\bar{a}_u = 1$. The electron beam has mean energy $E = 4.088$GeV, energy spread of $\Delta\gamma/\gamma = 0.001\%$, a normalized emittance of $\epsilon_n = 0.5\mu$m, with a mean beam radius in the focusing channel of approximately 30μm, and a peak current of $I_{pk} = 1.44$kA. The undulator modules are 100 periods long, of period $\lambda_u = 4$cm, with a drift between undulator modules of 0.5m. This corresponds to a total relative slippage between electrons and radiation in the undulator-drift sections of $108\lambda_r$. HGHG modulation is made at the 108^{th} subharmonic of λ_{r0}. Figure 3 shows the simulation results with the output exhibiting a linear frequency chirp with a relatively small temporal modulation of the output. The scheme appears to be robust to the 3D effects of diffraction and electron beam emittance. There is a clear repetitive linear correlation in the temporal-frequency analysis, separated by small breaks corresponding to the drift sections between the undulator modules.

4. Conclusion

The FM-FEL has been shown to exhibit similar properties to that of its conventional laser counterpart. It is a more complex system to study due to the relative temporal slippage of the radiation field through the co-propagating electron beam. FM-FEL operation has favourable scaling into the X-Ray regime, where only relatively small changes of the undulator parameter within each module are needed for a significant extension of the mode-amplification bandwidth

Optics EXPRESS

over that of a typical FEL. It has been demonstrated that it is possible to seed the FM-FEL interaction via harmonic lasing schemes e.g. HGHG, EEHG, or other methods where the bunching spectra exhibits a plateaux of harmonics/modes. The use of chicanes between the tapered undulator modules may also allow further control of the the modes [4], such as independent control of both the modal amplification bandwidth and spacing. These methods could lead to a powerful, tunable, broadband source of multi-coloured coherent radiation into the hard X-ray.

It is noted that the general concepts and methodology used here may also be valid and applicable within certain limits, to similar cooperative many-body systems, such as the Collective Atomic Recoil Laser (CARL) instability [19].

Funding

Science and Technology Facilities Council (Agreement Number 4163192 Release #3); ARCHIE-WeSt HPC, EPSRC grant EP/K000586/1; EPSRC Grant EP/M011607/1; John von Neumann Institute for Computing (NIC) on JUROPA at Jülich Supercomputing Centre (JSC), project HHH20.

Disclosures

The authors declare that there are no conflicts of interest related to this article.

References

1. P. Emma, R. Akre, J. Arthur, R. Bionta, C. Bostedt, J. Bozek, A. Brachmann, P. Bucksbaum, R. Coffee, F. J. Decker, Y. Ding, D. Dowell, S. Edstrom, A. Fisher, J. Frisch, S. Gilevich, J. Hastings, G. Hay, D. Schultz, T. Smith, P. Stefan, H. Tompkins, J. Turner, J. Welch, W. White, J. Wu, G. Yocky, and J. Galayda, "First lasing and operation of an Ångstrom-wavelength free-electron laser," Nat. Photonics **4**, 641–647 (2010).
2. T. Ishikawa, H. Aoyagi, T. Asaka, Y. Asano, N. Azumi, T. Bizen, H. Ego, K. Fukami, T. Fukui, Y. Furukawa, S. Goto, H. Hanaki, T. Hara, T. Hasegawa, T. Hatsui, A. Higashiya, T. Hirono, N. Hosoda, M. Ishii,T. Inagaki, Y. Inubushi, T. Itoga, Y. Joti, M. Kago, T. Kameshima, H. Kimura, Y. Kirihara, A. Kiyomichi, T. Kobayashi, C. Kondo, T. Kudo, H. Maesaka, X. M. Maréchal, T. Masuda, S. Matsubara, T. Matsumoto, T. Matsushita, S. Matsui, M. Nagasono, N. Nariyama, H. Ohashi, T. Ohata, T. Ohshima, S. Ono, Y. Otake, C. Saji, T. Sakurai, T. Sato, K. Sawada, T. Seike, K. Shirasawa, T. Sugimoto, S. Suzuki, S. Takahashi, H. Takebe, K. Takeshita, K. Tamasaku, H. Tanaka, R. Tanaka, T. Tanaka, T. Togashi, K. Togawa, A. Tokuhisa, H. Tomizawa, K. Tono, S. Wu, M. Yabashi, M. Yamaga, A. Yamashita, K. Yanagida, C. Zhang, T. Shintake, H. Kitamura, and N. Kumagai, "A compact X-ray free-electron laser emitting in the sub-Ångström region," Nat. Photonics **6**, 540–544 (2012).
3. B. W. J. McNeil and N. R. Thompson, "X-ray free-electron lasers," Nat. Photonics **4**, 814–821 (2010).
4. N.R. Thomson and B.W.J. McNeil, "Mode-Locking in a Free Electron Laser Amplifier," Phys. Rev. Lett. **100**, 203901 (2008).
5. D.J. Dunning, B.W.J. McNeil, and N.R. Thompson, "Few-Cycle Pulse Generation in an X-Ray Free-Electron Laser," Phys. Rev. Lett., **110**, 104801 (2013).
6. E. Kur, D.J. Dunning, B.W.J. McNeil, J. Wurtele, and A.A. Zholents, "A wide bandwidth free-electron laser with mode locking using current modulation," New J. Phys. **13**, 063012 (2011).
7. L.T. Campbell, B.W.J. McNeil, and S. Reiche, "Two-colour free electron laser with wide frequency separation using a single monoenergetic electron beam," New J. Phys. **16**, 103019 (2014).
8. A. Marinelli, A. A. Lutman, J. Wu, Y. Ding, J. Krzywinski, H.-D. Nuhn, Y. Feng, R. N. Coffee, and C. Pellegrini, "Multicolor Operation and Spectral Control in a Gain-Modulated X-Ray Free-Electron Laser," Phys. Rev. Lett. **111**, 134801 (2013).
9. R. Bonifacio, C. Pellegrini, and L.M. Narducci, "Collective instabilities and high-gain regime in a free electron laser," Opt. Comm. **50**, 373–378 (1984).
10. A.E. Siegman, *Lasers* (University Science Books, 1986).
11. R. Bonifacio, F. Casagrande, M. Ferrario, P. Pierini, and N. Piovella, "Hamiltonian model and scaling laws for free-electron-laser amplifiers with tapered wiggler," Opt. Comm. **66**, 133–139 (1988).
12. R. Bonifacio, B.W.J. McNeil, and P Pierini, "Superradiance in the High-Gain Free Electron Laser," Phys. Rev. A **40**, 4467–4475 (1989).
13. L.T. Campbell and B.W.J. McNeil, "Puffin: A three dimensional, unaveraged free electron laser simulation code," Phys. Plasmas **19**, 093119 (2012).
14. L.H. Yu, "Generation of intense uv radiation by subharmonically seeded single-pass free-electron lasers," Phys. Rev. A **44**, 5178–5193 (1991).

Optics EXPRESS

15. G. Stupakov, "Using the Beam-Echo Effect for Generation of Short-Wavelength Radiation," Phys. Rev. Lett. **102**, 074801 (2009).
16. I. Daubechies, J. Lu, and H.T. Wu, "Synchrosqueezed wavelet transforms: An empirical mode decomposition-like tool," Appl. Comput. Harmon. Anal. **30**, 243–261 (2011).
17. P. R. Ribič, E. Roussel, G. Penn, G. De Ninno, L. Giannessi, G. Penco, and E. Allaria, "Echo-Enabled Harmonic Generation Studies for the FERMI Free-Electron Laser," Photonics **4**, 19 (2017).
18. Paul Scherrer Institut, Athos Conceptual Design Report, 17-02 (2017).
19. R. Bonifacio and L. De Salvo, "Collective atomic recoil laser (CARL) optical gain without inversion by collective atomic recoil and self-bunching of two-level atoms," Nucl. Instrum. Methods Phys. Res. A **341**, 360–362 (1994).